Evolutionary Path Planning for Autonomous Underwater Vehicles in a Variable Ocean

Alberto Alvarez, Andrea Caiti, and Reiner Onken

***Abstract*—This paper proposes a genetic algorithm (GA) for path planning of an autonomous underwater vehicle in an ocean environment characterized by strong currents and enhanced space–time variability. The goal is to find a safe path that takes the vehicle from its starting location to a mission-specified destination, minimizing the energy cost. The GA includes novel genetic operators that ensure the convergence to the global minimum even in cases where the structure (in space and time) of the current field implies the existence of different local minima. The performance of these operators is discussed. The proposed algorithm is suitable for situations in which the vehicle has to operate energy-exhaustive missions.**

***Index Terms*—Autonomous underwater vehicles (AUVs), genetic algorithms, ocean variability, optimization, path planning.**

I. Introduction

PATH PLANNING that optimizes certain aspects of the vehicle's performance is a fundamental requirement for autonomous vehicles [17]. In autonomous underwater vehicles (AUVs), the aspects to be optimized have been related to traveling time and safety conditions. The path should be devoided of known obstacles or hazardous areas. This works well when energy considerations are negligible; however, concerns arise when vehicles have to operate energy-exhaustive missions in environments characterized by comparatively strong currents and complex spatiotemporal variability. In such cases, it is of primary importance to plan safety routes with a minimum energy cost. An example of such an approach can be found in [2], where AUV mission planning is proposed in order to optimize energy consumption while guaranteeing spatio-temporal coverage in oceanographic sampling. A different problem has been investigated in [11], where the optimization problem is formulated as a shortest path problem, guaranteeing terrain coverage with a sonar system over a given area. In recent years, interests in oceanography have moved toward littoral waters, where the marine environment is particularly variable in space and time [23]. Underwater vehicles usually encounter strong current fields in these regions. In such circumstances, mission planning that optimizes the energy cost would be highly desirable. This could be accomplished by incorporating information on the environmental space–time variability into existing path-finding algorithms.

Several approaches to solving the path-finding problem can be found in the literature [14]. Based on when the path is produced, path-finding algorithms can be divided into pregenerative and reactive. While in the first class the planning is carried out prior to the mission, with no course corrections [7], in the reactive class of algorithms the path is found by the vehicle as it proceeds through the environment [16]. Different computational methods are employed by existing path-planning algorithms. Potential field algorithms use artificial potential fields applied to the obstacles and goal positions and use the resulting field to influence the path of the robot [28]. These methods are fast and can be extended to higher dimensions, but are susceptible to local minima. The graph-searching techniques are so named because a chart or graph is produced, showing free spaces where no collision will occur and forbidden spaces where a collision will occur. Based on this graph, a path is selected by piecing together the free spaces or by tracing around the forbiden spaces [5]. Graph-searching approaches are robust to local minima solutions, but are difficult to employ in high-dimension problems. Dynamic programming [4] is usually employed as a graph-searching procedure when a cost is associated to each arc of the graph. While able to produce the optimal solution, the computational time of dynamic programming is proportional to the number of nodes in the graph, which in turn is dependent on the gridding (finer, coarser) of the solution space and increases geometrically with the dimension of the solution space. In the case of AUV navigation in space- and time-varying environments, the solution space is a four-dimensional (4-D) space and dynamic programming may not be computationally feasible, particularly in the reactive path-planning case, in which the optimal path is recomputed each time the information on the environment is updated. Techniques such as case-based reasoning have also been applied to the path-planning problem [27].

The application to path planning of a search procedure based on the Darwinian theories of natural selection and survival has been recognized [10], [13], [19]. In these strategies, called genetic algorithms (GAs), a population of possible paths is maintained and the paths are iteratively transformed by genetic operators such as crossover and mutation. GAs have been applied to the path-planning problem of terrain and underwater mobile robots [12], [19], [26], [9]. Unlike dynamic programming, the computational complexity of soft-computing optimization methods, as GAs, increases linearly with the dimension of the solution space (i.e., logarithmically with the number of nodes) [15]. Their drawback is that convergence to the optimal

Manuscript received January 7, 2002; revised November 26, 2003.

A. Alvarez was with the North Atlantic Treaty Organization, SACLANT Undersea Research Centre, La Spezia 19138, Italy. He now is with the Instituto Mediterraneo de Estudios Avanzados (CSIC-UIB), Esporlas 07190, Spain.

A. Caiti is with the Interuniversity Center Integrated Systems for the Marine Environment (ISME) and Department of Electrical Systems and Automation (DSEA), University of Pisa, Pisa 56100, Italy.

R. Onken was with the North Atlantic Treaty Organization, SACLANT Undersea Research Centre, La Spezia 19138, Italy. He is now with the Institute of Coastal Research (GKSS), Geesthacht D-21502, Germany.

Digital Object Identifier 10.1109/JOE.2004.827837

solution is not guaranteed in finite time, so that one may end up with a suboptimal solution. Previously proposed GAs for path planning of underwater vehicles have not taken into account the space–time variable nature of the surrounding environment.

In this study, we introduce a GA for the path-planning problem of underwater vehicles incorporating the space–time variability of the ocean environment. Prediction of the temporal evolution of the oceanographic conditions can be generated by forecast models or can be acquired as the vehicle navigates, by incorporating new measurements and updated forecasts. Hence, the planning algorithm can be applied without modification in mixed pregenerative/reactive planning situations. The proposed approach combines the use of special operators in the GA procedure, leading to better robustness and convergence properties. Moreover, the algorithm proposed in the three-dimensional (3-D) space- and time-varying case (in which the solution space is 4-D) is a hybrid algorithm, incorporating both dynamic programming on reduced-dimension subspaces and GAs. Preliminary results on this line of research, restricted to the two-dimensional (2-D) case, have been presented in [1]. In this work, a complete and detailed description of the algorithm and its performance in a 3-D space- and time-variant setting is provided, together with its application to a real environmental situation in the Mediterranean Sea. This paperis organized as follows. Section II defines the path-planning problem to be solved and describes the major characteristics of the proposed GA algorithm. Section III shows the results obtained for different configurations of the GA algorithm in different representative cases: a stationary ocean with a complex spatially variable current field and a space–time variable situation, in 2-D and 3-D cases. Section IV describes the results of applying the GA algorithm to optimize the energy cost of the path of an hypothetical AUV in a real ocean environment. Section V gives concluding remarks.

II. Path-Planning Problem

Consider an underwater environment discretized in space over an $m \times n \times p$ regular grid along the three Cartesian directions, assuming $z = 0$ at the sea surface, and the z-axis directed toward the sea bottom. Let $\Delta x, \Delta y, \Delta z$ be the gridding intervals in the x, y, z, respectively, axis. Any point in the grid defines a node $\mathbf{x} = (h, k, j), 0 \le h < m, 0 \le k < n, 0 \le j < p$. A path Γ between a starting node $\mathbf{s}$ and a destination node $\mathbf{d}$ is defined through a sequence of nodes $\Gamma = \{\mathbf{s}, \ldots, \mathbf{x}_i, \mathbf{x}_{i+1}, \cdots, \mathbf{d}\}$ and is made by straight-line segments connecting any two adjacent nodes $\mathbf{x}_i, \mathbf{x}_{i+1}$. In practice, it is assumed that the AUV navigation is defined through waypoints that are the nodes of the grid. Obstacles (such as varying bathymetry or coastlines) can be inserted by marking some of the nodes as "unfeasible." A current velocity vector $\mathbf{v}_c(x, y, z)$ is defined at any point in space. Within this setting, the path-planning problem can be enunciated as follows: given a start node $\mathbf{s}$ and a destination node $\mathbf{d}$, obstacles and current fields, find a path such that the energy cost required for a vehicle traveling along the path at a constant speed c is minimum, subject to the constraints that the path does not intersect any solid obstacle.The assumption of constant AUV speed with respect to the bottom corresponds to finding the path that will meet the mission requirements with less energy consumption. Other optimization problems, such as finding the minimum-time path with a given thrust power, could be solved by the technique developed in this work, after proper modification of the cost function. For simplicity, we will assume that $m = n = p$ and that the start and destination nodes define the beginning and ending coordinates in the x-axis, i.e., $\mathbf{s} = (0, \cdot, \cdot), \mathbf{d} = (m-1, \cdot, \cdot)$. All paths will be considered strictly monotone with respect to the x-coordinate and such that any two adjacent nodes $\mathbf{x}_i, \mathbf{x}_{i+1}$ satisfy the relation $h_{i+1} = h_i + 1$. This implies that each admissible path is a sequence of m nodes. Obviously, not all paths are monotone. Thus, this assumption could imply the possibility of excluding an optimum path in ocean areas with extremly crowded obstacles. However, monotone paths are reasonably powerful to express complicated paths when the space gridding is not dense [26]. Moreover, in a variable ocean, constraints to monotone paths and adequate constant cruise speed naturally avoid undesired solutions that involve backward drifting of the vehicle by the ocean currents. The proposed GA algorithm to solve the above enunciated path-planning problem consists of a few simple routines, as follows.

1) *Initialization.* A population of N individuals is randomly generated, where each individual corresponds to a candidate solution path and the population is a collection of such potential solutions. All the paths in the population are generated as random walks joining the starting and ending nodes.
2) *Computing the strength of the individuals.* The energy cost required to run each path of the initial population is evaluated; this is carried out by computing and adding up the energy required to overcome the drag generated by the current field in each segment constituting a determined path. Consider the ith segment $X_{i-1}X_i$ connecting the nodes $\mathbf{x}_{i-1}, \mathbf{x}_i$ of any arbitrary path. Let d_i indicate its length and let $\mathbf{e}_i$ be a unitary vector oriented along the segment $X_{i-1}X_i$ in the direction of the desired motion of the vehicle. Since it is required that the vehicle moves along the segment at the nominal speed c, at any point (x, y, z) along the segment the vehicle must have a velocity $\mathbf{v}_i(x, y, z)$ given by

$$\mathbf{v}_i(x, y, z) = c\mathbf{e}_i - \mathbf{v}_c(x, y, z) \quad (x, y, z) \in X_{i-1}X_i. \tag{1}$$

Consider the quantity

$$J_i = \iiint_{X_{i-1}X_i} \|\mathbf{v}_i(x, y, z)\|^3 \, dx \, dy \, dz. \tag{2}$$

Then, the energy cost W_i for the ith segment is given by

$$W_i = \frac{\rho J_i}{c} \tag{3}$$

where ρ is a constant depending on the dimensions of the vehicle and water properties. The total cost of a given path is finally given by the summation $\sum_i^m W_i$. Those paths with unfeasible nodes are heavily penalized with an extra

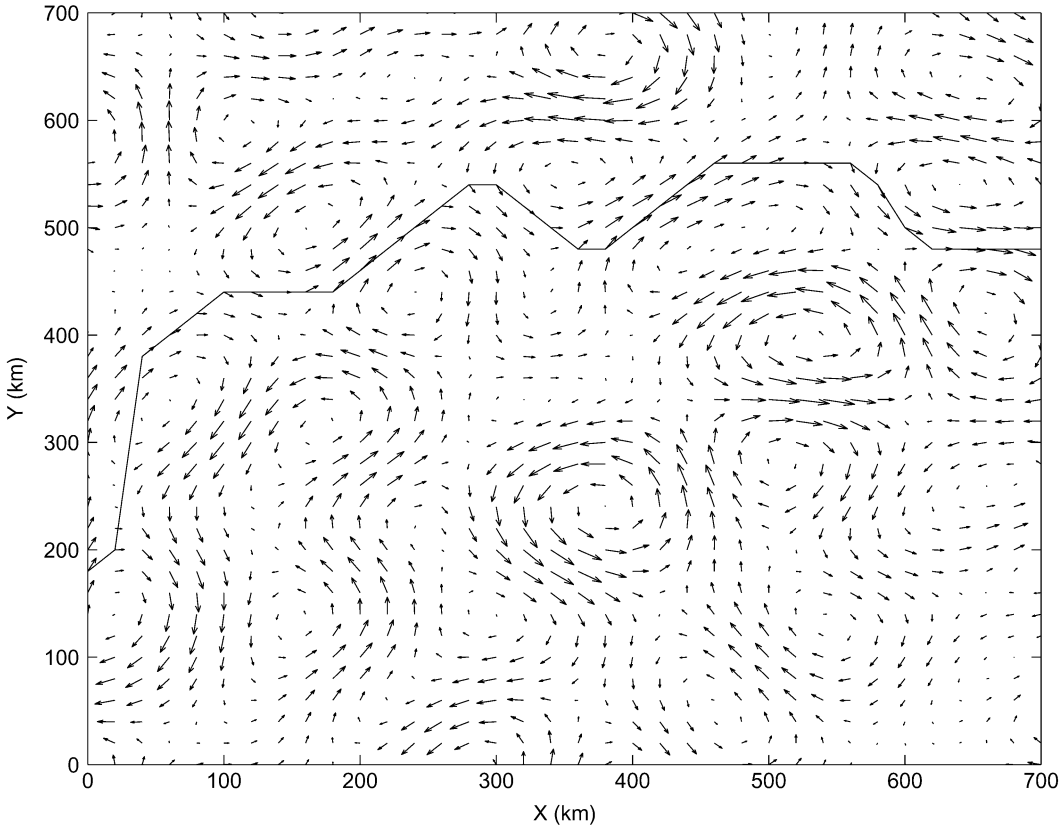

Fig. 1. Current field and optimum path from left to right.

energy cost. Note that, for optimization purposes, the cost can be computed directly by adding up the J_i, instead of the W_i, since the term J_i contains the only variable terms that influence the cost, i.e., the true vehicle velocity $\mathbf{v}_i$ and the segment length. In practical implementation, the computation of J_i is carried out as a finite summation over a grid of points that may or may not coincide with the grid of waypoint nodes. The strength of the path is defined in relative terms with respect to the other paths through its energy cost. Those paths with the lowest energy are the strongest.

3) *Selection.* The $\mathrm{N}/2$ individuals with lowest energy cost (strongest) are chosen from the current population.
4) *Crossover.* New individuals (called offspring) are produced from the selected paths by applying a crossover operator. A mate for each path is randomly selected from the $\mathrm{N}/2$ individuals. Thus, a total of $\mathrm{N}/4$ pairs are formed. The first two offspring of each pair are identical to their parents. The two other offspring are formed as recombinations of their parents. With the first two offspring, the best potential solutions are preserved, while provisions for improvement are made with the second pair of offspring. The recombination process between two selected paths is defined by the following steps: first, each x-monotone path is represented by a column-wise (or row-wise) sequence of m triads of x, y and z coordinates. x-coordinates h_1 and h_2 are randomly chosen from the finite set of integers uniformly distributed in the open intervals $(0, m-1)$ and (h_1, m), respectively. Offspring are generated by interchanging between the parents' individuals the y and z-coordinates of those nodes with an x-coordinate in the interval (h_1, h_2).
5) *Mutation.* A small percentage of paths is mutated at random. Specifically, during mutation a determined number of paths are randomly selected. For a selected path, x-coordinates h_1 and h_2 are randomly chosen in the open intervals $(0, m-1)$ and (h_1, m), respectively. Changes are applied to the y and z-coordinates of nodes with x-coordinate belonging to the interval (h_1, h_2). Specifically, nodes are changed to $\mathbf{x}_{\mathrm{new}} = (h, k+\delta_y, j+\delta_z)$ where δ_y and δ_z are integers randomly chosen from the intervals $[-\Delta_y, \Delta_y]$ and $[-\Delta_z, \Delta_z]$, respectively. The top-ranked paths are exempted from mutation, so that their information is not lost inadvertently. Mutation ensures that the solutions do not converge prematurely to a stable local minimum. The number of mutations in each generation, the percentage of paths that are exempted, and the interval size Δ_y, Δ_z are parameters that must be specified at the outset.

Parts (b)–(e) of the algorithm are reiterated for a certain number of generations or until a stop criterion is satisifed. Several local minima close to the optimum can appear, depending on the structure of the current field. In general, standard GAs that use a strong selection policy and small mutation rates quickly eliminate diversity from the population, as they seek out a global minimum. This loss of diversity in the population, in conjunction with deviations from isotropic statistics in the initial randomly generated population, can drive the GA toward

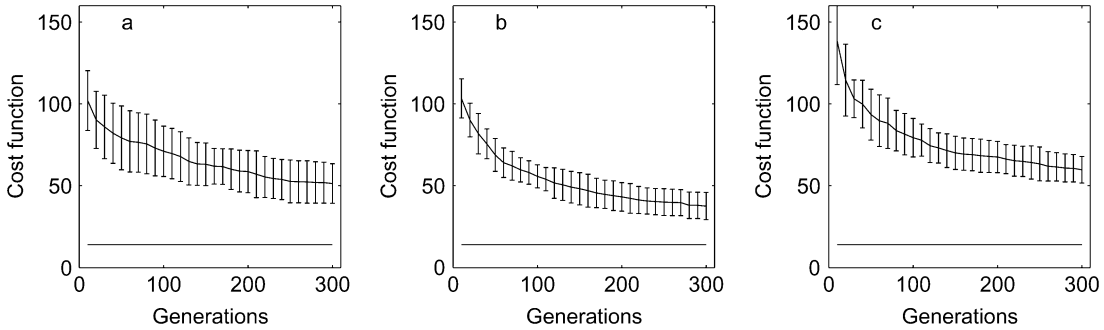

Fig. 2. Evolution of the cost function of the best path of each generation, averaged over an ensemble of ten simulations, for standard GA with mutation rates of (a) 0.05, (b) 0.25, and (c) 0.75. The straight line is the minimum value obtained by dynamic programming.

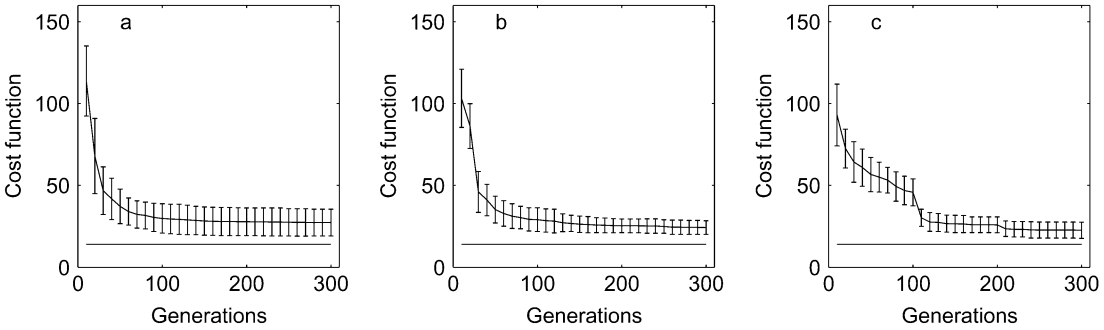

Fig. 3. Evolution of the cost function of the best path of each generation, averaged over an ensemble of ten simulations, for standard GA and random immigrants introduced every (a) 10 , (b) 20, and (c) 100 generations. The straight line is the minimum value obtained by dynamic programming.

suboptimal solutions. To avoid this, two operators have been incorporated into the implemented GA. The first, called iteration [19], consists of running the GA several times from different initial conditions and a few generations. The best individual of each run is selected to form part of the initial population of the definitive run. The role of the iteration operator here is not that of multimodal optimization, but to provide gross estimations of the possible minima to the initial population. A second genetic mechanism has been incorporated in the proposed algorithm. This operator is based on the random immigrants mechanism [8], which originally replaces part of the population at each generation with randomly generated values. The operator is employed to substitute, after a certain number of generations, the individuals of the population by random perturbations of the strongest individual. The level of randomness is determined by the degree of diversity of the evolving population.

III. Results

A. Sensitivity and Robustness of the GA Algorithm: Performance in a 2-D Stationary Environment With Complex Spatial Variability

The performance of the developed GA algorithm is first studied in a simple case described by a 2-D stationary ocean environment showing complex spatial variability, to assess its sensitivity and robustness to different parameters. The GA algorithm described has been implemented for path planning in a 2-D spatial domain represented by a grid of 36×36 points. The distance between grid points corresponds to 20 km, so that the total system size is $L = 700$ km. A stationary current field with complex spatial variability (Fig. 1) has been randomly generated from a specific isotropic power spectrum with random phases. Velocities in the current field are of the order of 0.5 ms^{-1}. No obstacles have been considered in the domain. As a reference, the optimum solution has been computed using dynamic programming (Fig. 1).

The GA has been configured in such a way that the population size is 100 individuals and the stopping criterion is given by an upper limit of 300 generations and $\Delta_y = \Delta_z = 3$. Fig. 2(a)–(c) shows the evolution of the cost function of the best path of each generation, averaged over an ensemble of ten simulations, for a standard GA configuration, i.e., without iteration and random immigrants operators and with mutation probabilities of 0.05, 0.25, and 0.75, respectively. The result shows an average decrease of the cost function with the generations for all cases. For low mutation rates [Fig. 2(a)] the random search component of the GA represented by mutation is rather limited, leading the crossover mechanism to search through the space of possible solutions. The deterministic nature of crossover implies a major dependence of the final result on the initial population as well as a major sensitivity versus the existence of local minima. Both aspects translate into high values of the standard deviations obtained from the ensemble statistics. Conversely, mutation leads the searching procedure in the GA for high mutation probabilities [Fig. 2(c)]. The algorithm gains robustness to the existence of local minima, but its convergence is slower, resembling pure random search procedures. Best performance of the GA algorithm has been found numerically for mutation rates ranging from 0.15 to 0.5. Fig. 2(b) shows the results obtained with a mutation rate of 0.25. Although the result substantially improves the ones obtained in the previous cases, the minimum value achieved by the algorithm is still far from the real optimal

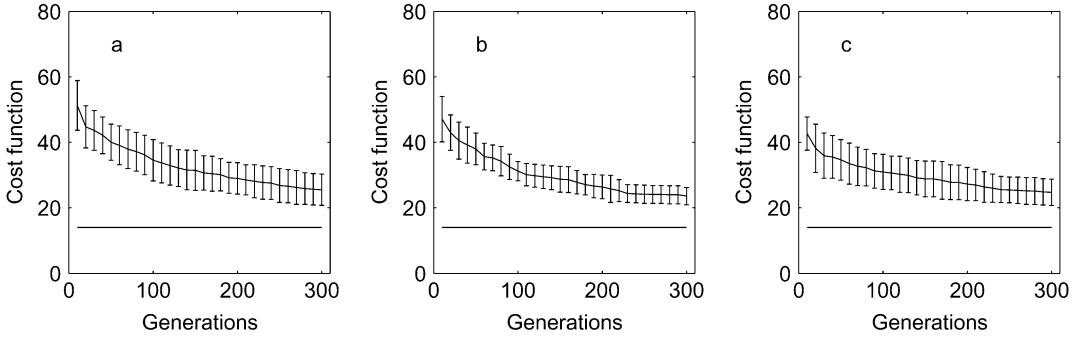

Fig. 4. Evolution of the cost function of the best path of each generation, averaged over an ensemble of ten simulations, for standard GA and iteration. Best individuals to form part of the initial population of the final run have been selected after (a) 5, (b) 10, and (c) 20 generations. The straight line is the minimum value obtained by dynamic programming.

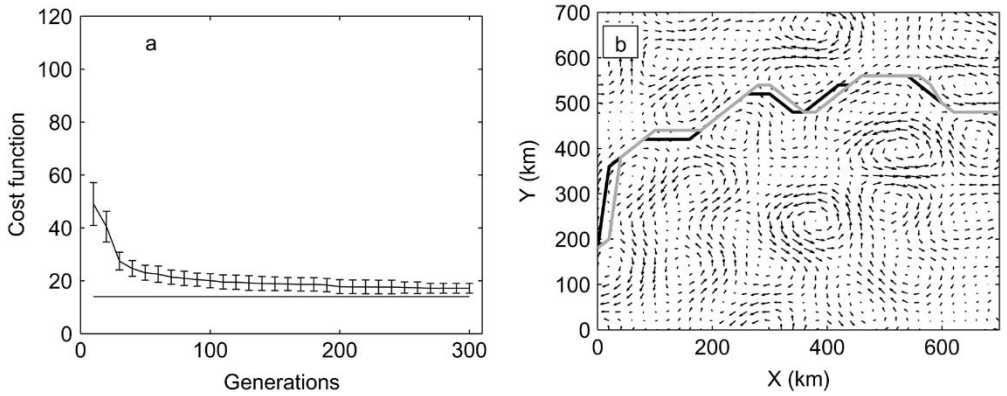

Fig. 5. (a) Evolution of the cost function of the best path of each generation, averaged over an ensemble of ten simulations, for standard GA including random immigrants and iteration operators. (b) Optimum paths obtained by the GA (black) and dynamic-programming (gray) approaches.

solution. The high values of the standard deviations obtained from the ensemble statistics indicate a lack of robustness of the algorithm. Different simulations will provide different paths with cost energies that will vary by $\pm 25\%$ of the mean ensemble value. A mutation rate equals 0.25 will be employed in the forthcoming simulations.

An ensemble of simulations have been carried out incorporating random immigrants every 10, 20, and 100 generations [Fig. 3(a)–(c), respectively]. Inclusion of random immigrants implies a clear improvement in the performance of the algorithm with respect to the standard version. Specifically, a sharp decrease is observed in Fig. 3(b) and (c) in the average evolution of the cost function after the operator has been applied at generations 20 and 100, respectively. Also notice the reducing tendency found in the computed standard deviations, implying a greater robustness of the algorithm than in the standard case. Hereafter, the hypermutation operator will be applied every 20 generations. Similarly to the previous simulations, a set of runs has been carried out, incorporating the iteration operator to the standard GA. Fig. 4(a)–(c) displays the results obtained when the iteration operator is applied to generate 20 individuals of the initial population, selecting the best individual after 5, 10, and 20 generations, respectively. Fig. 4 indicates that the inclusion of an iteration substantially improves the results obtained by the standard GA. The performance obtained by the algorithm is similar to that obtained when random immigrants are considered. The best result is obtained when the selection of the best individual occurs after 10 generations and, so, this value is employed when using iteration. Finally, Fig. 5(a) and (b) shows the results obtained when iteration and random immigrant operators are included in the standard GA. Excellent agreement is obtained with the result computed from dynamic programming.

Although the present study is mainly devoted to the problem of path planning in an ocean showing spatio-temporal variability, Fig. 6(a) and (b) shows the solution obtained by the developed GA including random immigrants and iteration operators when an obstacle is present. Notice that the obstacle is intentionally located to partially block the optimum trajectory found in the case without obstacles. Unlike classical obstacle-avoidance problems, the optimum path found by the algorithm in this case is not constituted by segments from the optimal path in absence of the obstacle in the unblocked area plus extra segments surrounding the obstacle. Instead and due to the considered spatial ocean variability, a new path that is very different from the optimal solution in the absence of the obstacle is found. The optimum path takes advantage of the advection of three eddy structures in the ocean [Fig. 6(b)]. This result exemplifies the richness introduced by the ocean spatial variability in a path-planning problem.

B. 2-D Space–Time Variability

A path-planing problem is now considered in a 2-D ocean environment showing space–time variability. The spatial domain is defined by a grid of 20×20 points. The space–time variable

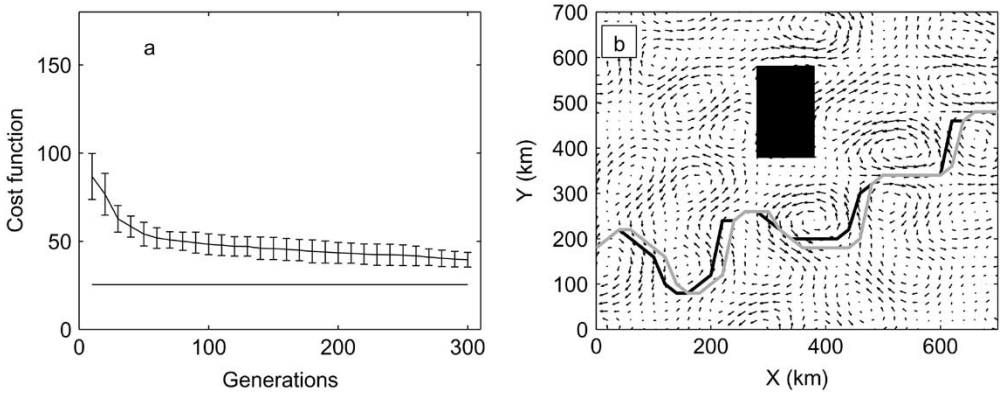

Fig. 6. (a) Evolution of the cost function of the best path of each generation, averaged over an ensemble of ten simulations, for standard GA including random immigrants, iteration operators, and obstacles. (b) Optimum paths obtained by the GA (black) and dynamic-programming (gray) approaches.

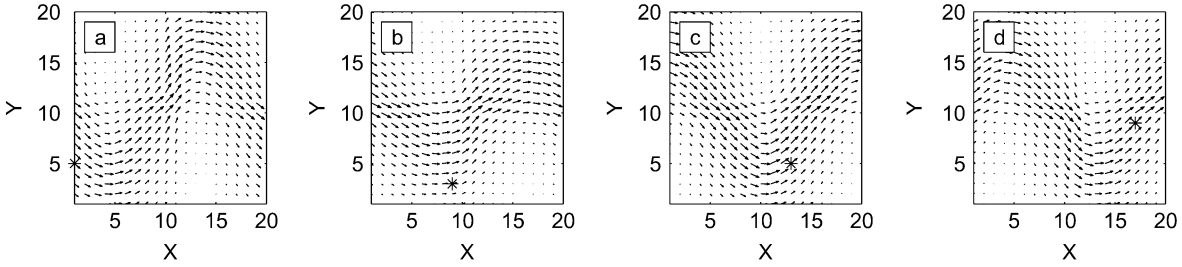

Fig. 7. Time sequence of the computed path planning for a virtual AUV (asterisk) in a space–time variable ocean jet.

current field is described by a jet flowing eastward with meanders in the north–south direction. These meanders are also advected by the jet at phase velocity c. A mathematical model for this flow is given by the streamfunction [3], [6]

$$\phi(x,y) = 1 - \tanh\left(\frac{y - B(t)\cos(k(x-ct))}{(1+k^2B(t)^2\sin^2(k(x-ct)))^{\frac{1}{2}}}\right) \quad (4)$$

where $B(t)$ and k are the properly adimensionalized amplitude and wavenumber of the undulation in the streamfunction. The specific expression for $B(t)$ is

$$B(t) = B_o + \epsilon\cos(\omega t + \theta) \quad (5)$$

with $B_o = 1.2, c = 0.12, k = 0.84, \omega = 0.4, \epsilon = 0.3$, and $\theta = \pi/2$. The velocity field is obtained from the streamfunction by the relations

$$U(x,y,t) = -\frac{\partial\phi}{\partial y} \quad V(x,y,t) = \frac{\partial\phi}{\partial x} \quad (6)$$

where $U(x,y,t), V(x,y,t)$ are, respectively, the x– and y-components of the velocity vector at time t in the location with adimensional coordinates (x,y). Adimensional velocity of the AUV has a value of 0.5. The current field is updated for each integer value of time $(t = 1, 2, \ldots)$. This mathematical model of ocean flow has been widely employed to study large-scale ocean chaos. In our case, the jet structure quickly varies on time scales of the same order of the vehicle's traveling time. This strong space–time variability is not common in large ocean flows, but represents an extreme situation that is useful for testing the performance of the algorithm. Starting and destination points are located at $(x = 1, y = 5)$ and $(x = 20, y = 12)$, respectively. No obstacles have been considered in this example. The standard GA algorithm and the random immigrant and iteration operators have been employed to solve the above-defined path-planning problem. A contribution of ten individuals has been provided by the iteration operator to the initial population, while random immigrants have been included at each generation. An evolutionary process with a total of 200 generations has been simulated. Fig. 7 shows a time sequence of the solution found by the algorithm. The path is synchronized with the time variability of the flow in such a way that the vehicle is always located in a position where the velocity field favors mission development.

C. 3-D Stationary Environment With Complex Spatial Variability

Unlike the atmospheric case, ocean environments are usually characterized by very weak vertical motions. This feature, together with the large extension of the horizontal dimensions by comparison with the vertical, results in a quasi-2-D nature on relatively small scales (few kilometers). In deep areas, ocean environments can be approximated by a layered structure with a well-defined circulation. In this section, we have considered the problem of path planning in a four-layered ocean. Fig. 8 shows the circulation patterns for each layer. Flow fields were randomly generated, similar to the 2-D case. The spatial domain corresponds to a grid of 36×36 points with a distance of 20 km between grid points corresponds. Eddy structures are order of 100 km with maximum velocities of $0.5\ \text{ms}^{-1}$.

The GA has been configured in such a way that the population size is 100 individuals and the stopping criterion is given by an upper limit of 600 generations. The mutation rate has been

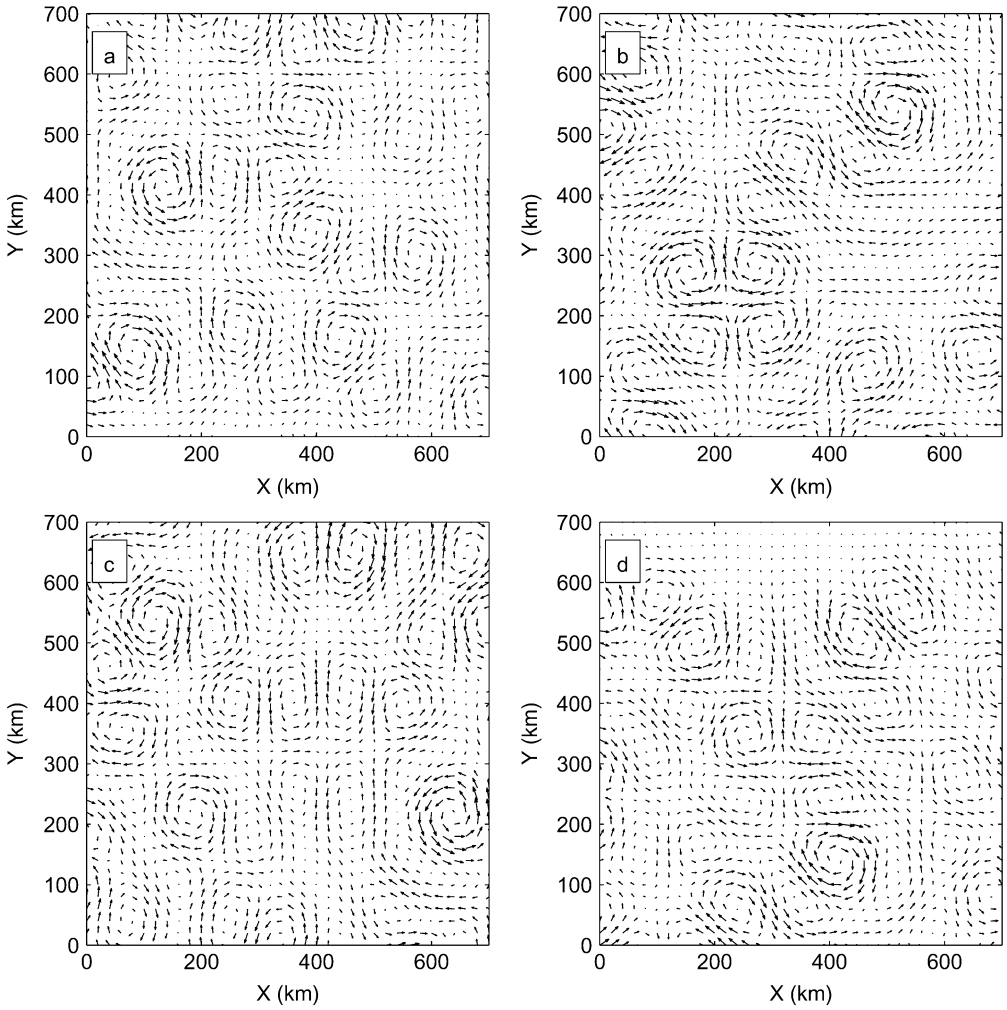

Fig. 8. Current field of the (a) first, (b) second, (c) third, and (d) fourth layers.

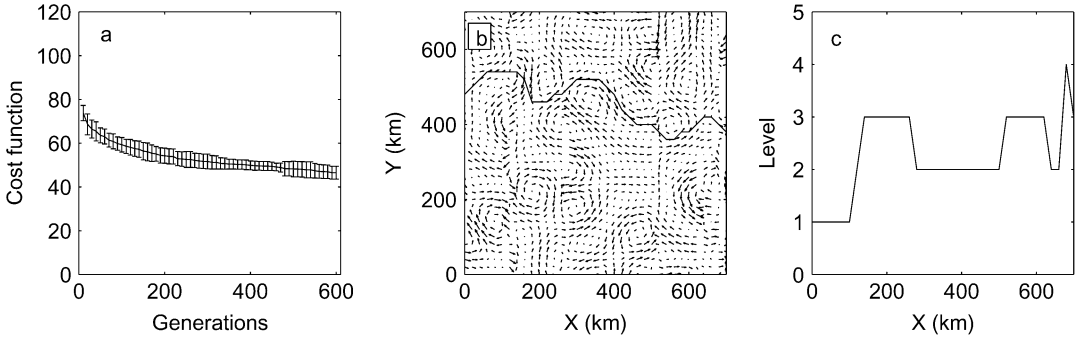

Fig. 9. (a) Evolution of the cost function in the 3-D case. (b) $x-y$ section of the 3-D path found by the GA. Notice that the displayed current field is a collage done with the velocities of the segments of each layer followed by the 3-D path. (c) $x-z$ section of the 3-D path.

fixed at 0.25. Finally, iteration and random immigrants operators have also been included. Random immigrants have been incorporated every 20 generations while the iteration operator has provided 20 individuals to the initial population. Fig. 9(a) shows the evolution of the cost function of the best path of each generation, averaged over an ensemble of ten simulations. The starting position is located in the first level while the final location lies in the third level. Fig. 9(b) displays an $x-y$ view of the best 3-D path found by the GA, superimposed on the effective current field obtained by plotting the current field of the layer prescribed by the path at each step. From this composition, it is possible to see how the path distributes among layers in order to get benefit of the currents to reach the final goal. These vertical movements are shown in Fig. 9(c).

Fig. 10 shows the results obtained with a slight modification in the working procedure of the GA. The initial population in this case has not been obtained with the iteration operator, but from computing with dynamic programming, the best 2-D paths for each layer. The 3-D paths were then built from the optimum 2-D paths by allowing random jumps among layers. In other

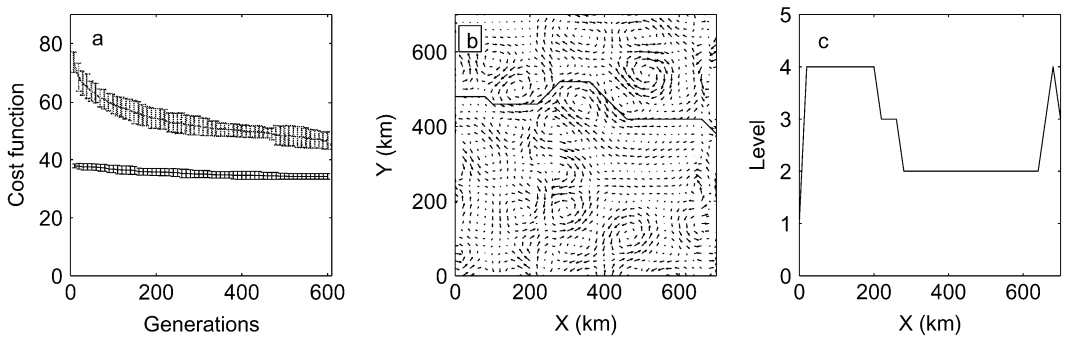

Fig. 10. Same as Fig. 9, but with the 3-D path found by the hybrid optimization algorithm. To facilitate comparison, the evolution of the cost function of the previous case is also displayed, shown in gray in (a).

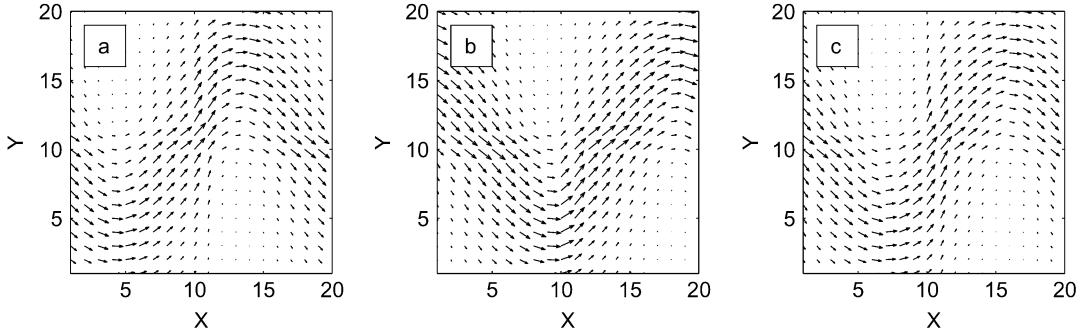

Fig. 11. Initial circulation pattern for the (a) first, (b) second, and (c) third layers in the space–time-variable 3-D ocean environment.

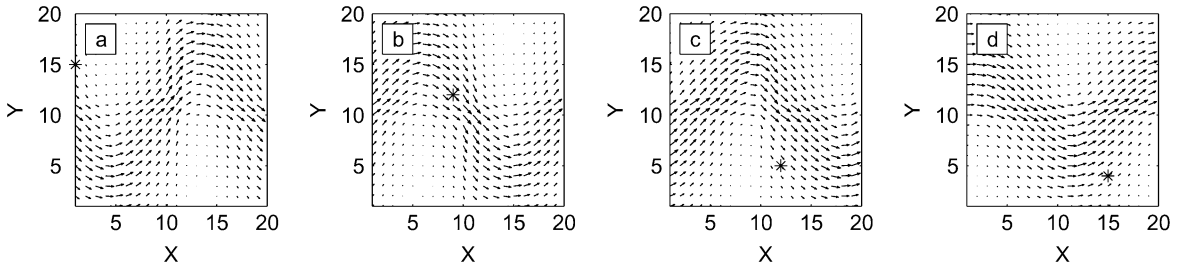

Fig. 12. Evolution of the cost function in the 3-D space–time variability.

words, the initial population of 3-D paths were in such a way that the movement in each layer is carried out following the optimum 2-D path, while improvements were introduced by selecting the layer at each step. The role of GA searching is then to find the combination of 2-D segments of the different layers that optimize the 3-D path to the destination point. Notice that this procedure reduces the dimensionality of the optimization problem, but the final 3-D path is not ensured to be the optimum. The point is to see if this approach that combines dynamic programming and GA improves the previous results. The improvement is shown in Fig. 10(a), with the lowering of the cost function with respect to the result shown in Fig. 9(a). Besides, fluctuations around the mean value also decrease, indicating that almost the same solution was achieved by the hybrid optimization algorithm in each one of the simulations of the ensemble. Fig. 10(b) displays an $x-y$ section of the 3-D path imposed on the collage done with the velocity fields, corresponding to the segments of each layer followed by the path. Finally, Fig. 10(c) shows an $x-z$ section of the 3-D path.

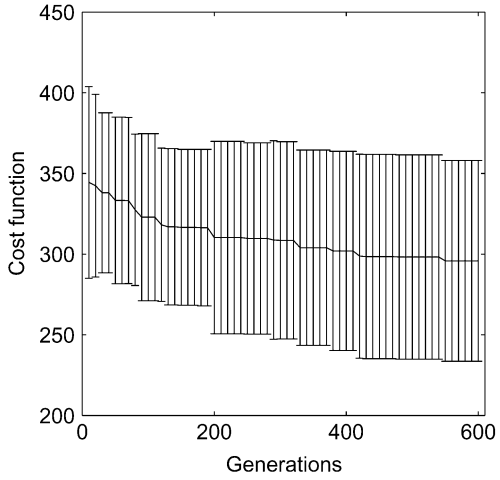

Fig. 13. Time sequence of the computed path planning for a virtual AUV (asterisk) in a space–time 3-D variable ocean.

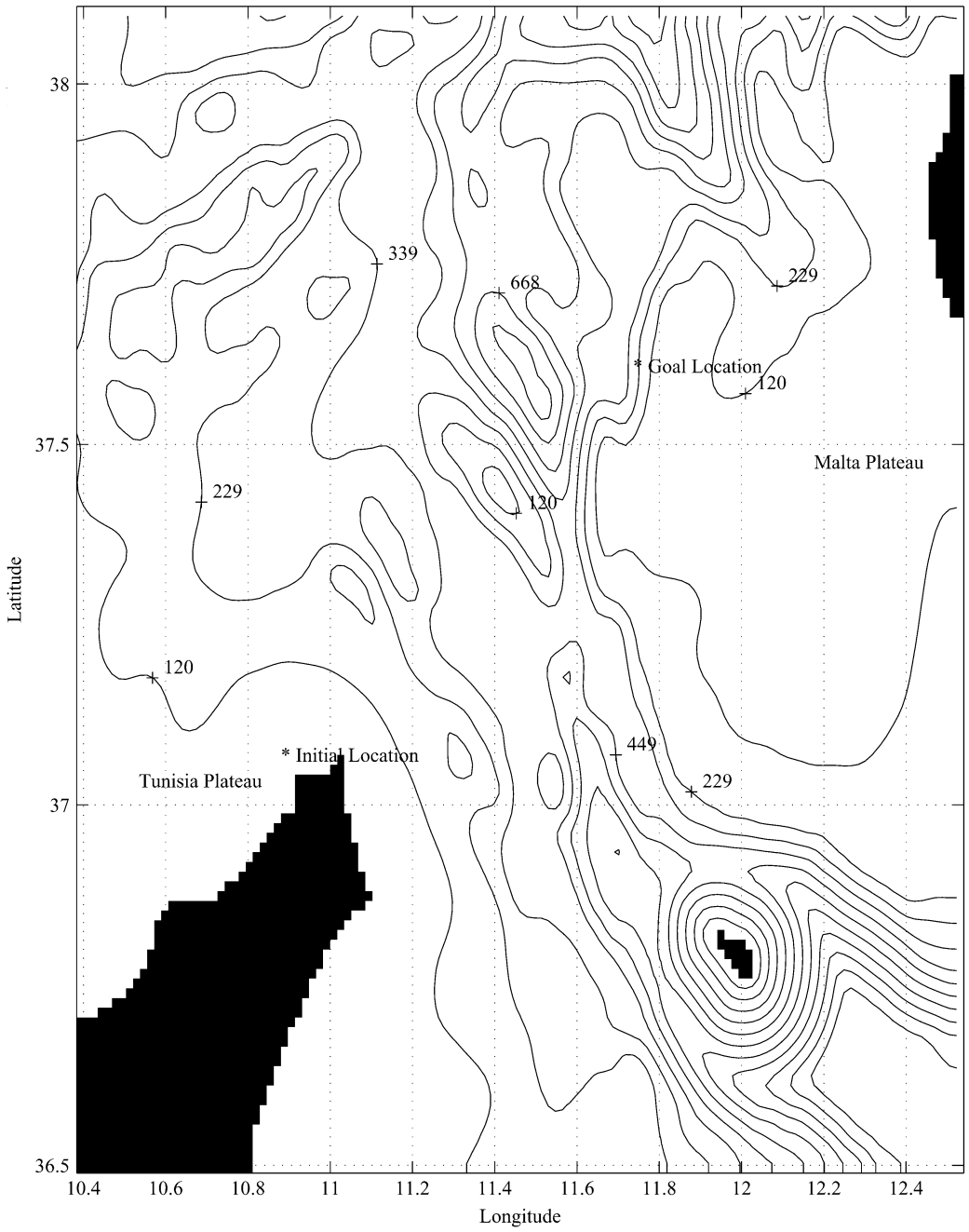

Fig. 14. Bathymetry of the Strait of Sicily. The initial location and destination points are also represented.

D. 3-D Space–Time Variability

An ocean environment showing space–time variability has finally been considered. The physical ocean environment is now characterized by three layers with a time-varying jet structure in each layer. The jets are found in different phases. Specifically, the form of the jet equation for each layer is given by

$$\phi(x,y) = 1 - \tanh\left(\frac{y - B(t)\cos(k(x-ct)+\alpha)}{(1+k^2B(t)^2\sin^2(k(x-ct)+\alpha))^{\frac{1}{2}}}\right) \tag{7}$$

with $\alpha = 0, \pi/2$, and $\pi/4$ for the first, second, and third layers, respectively. The remaining parameters and functions of the equation have been already defined in a previous section. Fig. 11 displays the initial circulation pattern for each of the layers. The starting position is located in the first layer, while the final one is in the third layer. As in the 3-D stationary case, vertical velocities have been neglected. Concerning the configuration of the GA, iteration and random immigrants operators have been included in the simulations. Their inclusion has been motivated by improvement of the results achieved with this configuration in previous cases. An ensemble of ten simulations with 600 generations each was carried out. Fig. 12 displays the evolution of the cost function of the best path of each generation, averaged over the ensemble. Notice that the possible final solution of the GA is less robust than in the stationary 3-D case, which is reflected in the high statistical error values. This feature is expected if we consider that now the optimization

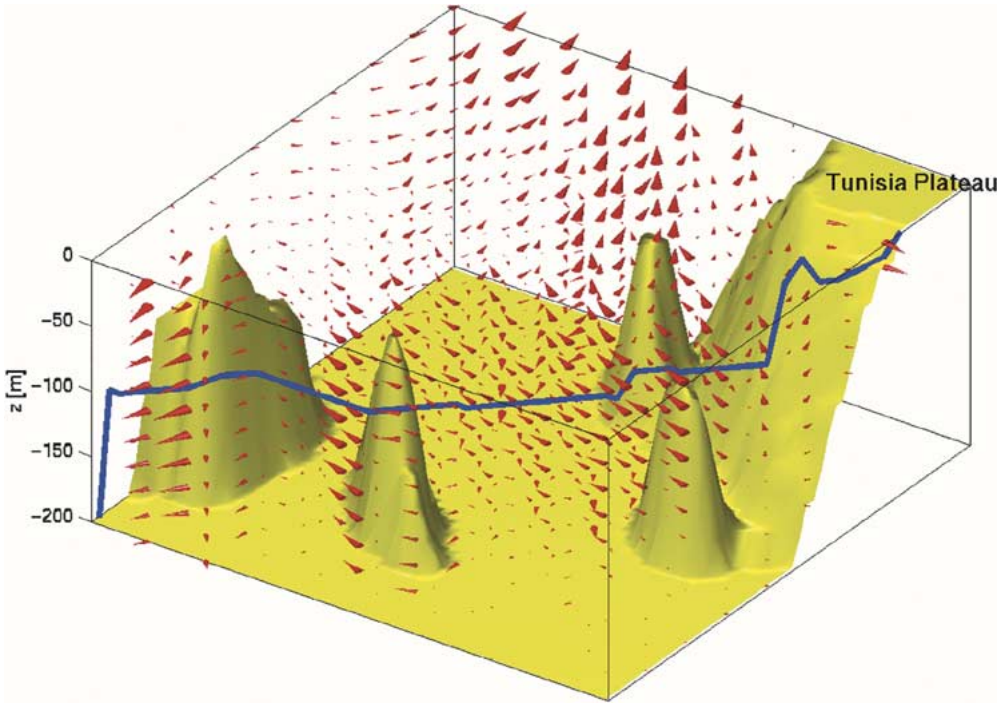

Fig. 15. Three-dimensional view of the batymetry current field and solution path.

problem is defined in four dimensions, three spatial and one temporal. Fig. 13 shows snapshots of the best 3-D trajectory found in the ensemble of simulations. At the beginning, the path develops in the first layer, where the starting position is located. Then, the trajectory jumps to the second layer. Notice from Fig. 11(b) that, due to the initial location, this layer would in principle be the best to develop the motion. Finally, the path moves to the third layer, where the destination point is located. The optimum 3-D path found by the GA roughly corresponds to what is expected; however, Fig. 13(a)–(c) shows that the selected path is not perfectly syncronized with the jet variability. In other words, the developed GA finds a 3-D path that is probably in the neighborhod of the optimum solution, but is suboptimal. As previously noted, difficulties to get the exact answer are induced by the high dimensionality of the optimization problem.

IV. Energy Optimization in a Near-to-Real Ocean Environment: Optimum Path to Cross the Sicily Channel

The GA algorithm previously developed is now employed to determine the path with minimum energy cost in a real 3-D ocean environment. The selected area for the simulation was the Sicily channel, located in the Mediterranean Sea (Fig. 14). The complex bathymetry and current fields characterizing this region were the main reasons for our election. Besides, oceanographic measurements in the channel have been recently carried out using the AUV AUTOSUB2 from Southampton Oceanographic Center, Southampton, U.K. [25].

In our experiment, bathymetry of the Sicily channel was obtained from the Data Bathymetric Data Base-Variable (DBDBV) Resolution of the Naval Oceanographic Office (http/128.160.23.42/dbdbv/dbdbv.htlm), providing a grid of 51×51 points with a horizontal resolution of 1.5 km. The current fields in the region were computed from the assimilation into a primitive equation numerical ocean model of conductivity-temperature-depth (CTD) casts from an hydrographic survey done in the area in October 1996 [20]. The Harvard primitive equation model [22] was employed for this purpose. The domain was divided into 35 vertical layers defined in terms of terrain-following σ coordinates [24], ranging from 3 m to the bottom. A detailed description of the oceanographic data assimilation and processing will be published elsewhere [21]. At the end, high-resolution current fields were obtained for depths ranging from 3 to 200 m with 20-m spacing. Restriction to the first 200 m was fixed to avoid excessive computation time. Besides, the most energetic and complex currents in the region are usually located in the first 200 m. Current fields have been considered to be stationary.

The configuration of the GA, which considers an initial population built from the optimum paths at each 2-D layer, has been employed to find a satisfying path between the deployment location at the surface in the Tunisia Plateau and the destination point located 200-m deep in the northern coast of Sicily (Fig. 15). The nominal velocity of the AUV is 1ms^{-1} while maximum current speeds are order of 0.65ms^{-1}. Fig. 15 displays a 3-D view of the current field, bathymetry, and the solution path obtained after 200 generations. The solution path implies an almost surface navigation in the first 7.5 km. Then, the path sinks to 80 m to continue the northeast navigation for another 10 km, passing under the strong surface current fields, adverse to the destination, and over a first topographic obstacle represented by an oceanic mountain. The path continues at a depth of 100 m surrounding a second topographic obstacle and finding a favorable current field near the coast of Sicily. Finally,

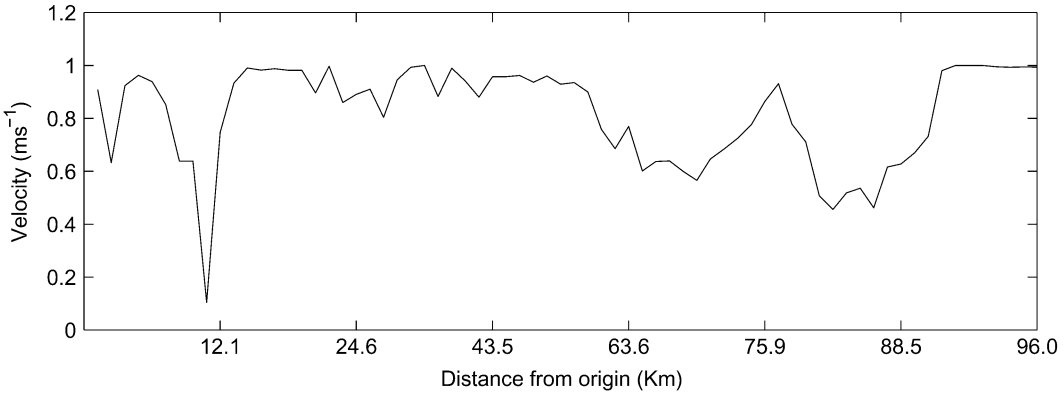

Fig. 16. Resulting velocity profile with respect to the water along the optimal path through the Strait of Sicily.

the path reaches the destination location at 200-m deep. Fig. 16 displays the resulting velocity profile with respect to the water along the optimal path. In some segments of the path, the vehicle has a velocity with respect to the water of 0.5 ms^{-1}. Although this is fine in terms of path planning, it could cause a substantial dynamic control problem. Since most AUVs do not have active ballast systems and are trimmed to be slightly positive, it is impossible to mantain control at such low speeds with respect to the water. Increasing the constant speed c would increase the power consumption, but a higher capability to control vehicle's depth and heading is gained.

V. Conclusion

Unlike other robotic systems, AUVs have to frequently operate in unknown ocean environments, characterized by a complex spatiotemporal variability. This variability can strongly perturb the proper development of an AUV's operations. Numerical ocean models can provide, to some extent, nowcasts and forecasts of the ocean currents. This information can be employed to improve the planning of missions, taking into account the variability of the environment. In this study, a GA has been developed to find the path with minimum energy cost in space–time-variable 2-D and 3-D ocean environments. A sensitivity study of the algorithm was carried out, considering the performance of the algorithm in 2-D and 3-D hypothetical environments. In the 2-D case, the characteristics of the path-planning problem allowed the comparison of the results obtained by the GA with that computed from traditional dynamic programming. The most robust results were obtained with the inclusion in the evolutionary process of two novel genetic operators, iteration and random immigrants. Next, the capability of the algorithm to provide mission planning in a space–time-variable environment was tested. Specifically, the algorithm successfully provided a consistent path for the navigation of an AUV in a 2-D space–time-variable ocean flow.

Simulations have also been carried out to test the performance of the GA in a fully 3-D case. In a 3-D stationary environment, best results were found by mixing the action of the GA with dynamic programming. This approach to find the optimum 3-D path is allowed if the ocean layers are not linked by the existence of vertical motions. This situation is quite common in the ocean, except on specific coastal areas where topographic irregularities, tidal currents, or upwelling can break this quasi-2-D behavior. Unlike in the 2-D case, there is no guarantee that the path found by the hybrid algorithm is the optimum, although the solution is generally robust. Difficulties increase when time variability is also included. In such circumstance, the results obtained with the GA seem to be near the optimum solution.

Finally, a near-to-real case simulation was carried out. This simulation was accomplished by the integration of the developed evolutionary algorithm with a numerical ocean model of the selected region. This region, the Sicily channel, is characterized by strong current fields and complex bathymetry. The GA algorithm provided an optimum path to cross the Sicily channel. This experiment addresses the possibility of using ocean prediction systems together with searching algorithms to find safe paths with minimum energy cost.

References

[1] A. Alvarez and A. Caiti, "A genetic algorithm for autonomous underwater vehicle route planning in ocean environments with complex space-time variability," in *Proc. Int. Federation Automatic Control (IFAC) Conf. Control Applications Marine Systems*, Glasgow, U.K., June 2001.

[2] J. G. Bellingham and J. S. Willcox, "Optimizing AUV oceanographic surveys," in *Proc. IEEE Symp. Autonomous Underwater Vehicles Technology*, Monterey, CA, 1996, pp. 391–398.

[3] F. S. Bower, "A simple kinematic mechanism for mixing fluid particles across a meandering jet," *J. Phys. Oceanogr.*, vol. 21, pp. 173–180, 1991.

[4] A. E. Bryson and Y. Ho, *Applied Optimal Control*. New York: Wiley, 1975.

[5] K. P. Carroll, S. R. McClaran, E. L. Nelson, D. M. Barnett, D. K. Friesen, and G. N. Williams, "AUV path planning: An A^* approach," in *Proc. IEEE Symp. AUV Technology (AUV'92)*, 1992, pp. 3–8.

[6] M. Cencini, G. Lacorata, A. Vulpiani, and E. Zambianchi, "Mixing in a meandering jet: A Markovian approximation," *J. Phys. Oceanogr.*, vol. 29, pp. 2578–2594, 1999.

[7] D. Z. Chen, R. J. Szczerba, and J. J. Urhan, "Planning conditional shortest paths through an unknown environment: A framed-quadtree approach," in *Proc. IEEE/RSJ Int. Conf. Intelligent Robots and System Human Interaction and Cooperation*, 1995, pp. 33–38.

[8] H. G. Cobb and J. J. Grefenstette, "Genetic algorithms for tracking changing environments," in *Proc. Int. Genetic Algorithms Conf.*, 1993, pp. 1–8.

[9] R. Fox, A. Garcia, and M. L. Nelson, "A three dimensional path planning algorithm for autonomous vehicles," in *Proc. 11th Int. Symp. Unmanned Untethered Submersible Technology*, 1999, pp. 546–556.

[10] D. E. Goldberg, *Genetic Algorithms in Search, Optimization and Machine Learning*. Boston, MA: Addison-Wesley, 1989.

[11] S. Hert, S. Tiwari, and V. Lumelsky, "A terrain-covering algortihm for an AUV," *J. Autonom. Robots*, no. 3, pp. 91–119, 1996.

[12] C. Hocaolglu and A. C. Sanderson, "Planning multi-paths using speciation in genetic algorithms," in *Proc. IEEE Int. Conf. Evolutionary Computation*, 1997, pp. 378–383.
[13] J. H. Holland, *Adaptation in Natural and Artificial Systems*. Ann Arbor, MI: Univ. of Michigan Press, 1992.
[14] Y. K. Hwang and N. Ahuja, "Gross motion planning—A survey," in *ACM Comp. Surveys*, 1992, pp. 219–291.
[15] J. S. R. Jang, C. T. Sun, and E. Mizutani, *Neuro-Fuzzy and Soft Computing—A Computational Approach to Learning and Machine Intelligence*. Englewood Cliffs, NJ: Prentice-Hall, 1997.
[16] I. Kamon and E. Rivlin, "Sensory based motion planning with global proofs," in *Proc. IEEE/RSJ Int. Conf. Intelligent Robots and System Human Interaction Cooperation*, 1995, pp. 435–440.
[17] J. C. Latombe, *Robot Motion Planning*. Amsterdam, The Netherlands: Kluwer, 1991.
[18] H. S. Lin, J. Xiao, and Z. Michalewicz, "Evolutionary algorithm for path planning in mobile robot environment," in *Proc. 1st IEEE Conf. Evolutionary Computation*, 1994, pp. 211–216.
[19] Z. Michalewicz, *Genetic Algorithms + Data Structures = Evolutionary Programs*. Berlin, Germany: Springer-Verlag, 1996.
[20] R. Onken and J. Sellschopp, "Water masses and circulation between the eastern Algerian basin and the Strait of Sicily in October 1996," *Oceanol. Acta*, vol. 24, pp. 151–167, 2001.
[21] R. Onken, A. R. Robinson, P. J. Haley, and L. A. Anderson, "Data-driven simulations of synoptic circulation and transports in the Tunisia-Sardinia-Sicily region," *J. Geophys. Res.*, vol. 108, pp. 8123–8136, 2003.
[22] A. R. Robinson, H. G. Arango, A. Warn-Varnas, W. G. Leslie, A. J. Miller, P. L. Haley, and C. J. Lozano, "Real-time regional forecasting," in *Modern Approaches to Data Assimilation in Ocean Modeling*. Amsterdam, The Netherlands: Elsevier, 1996, pp. 377–410.
[23] H. Schmidt and E. Bovio, "Underwater vehicle networks for acoustic and oceanographic measurements in the littoral ocean," in *Proc. 5th Int. Federation Automatic Control (IFAC) Conf. Manoeuvring Control Marine Craft (MCMC'00)*, 2000, pp. 323–326.
[24] M. A. Spall and A. R. Robinson, "A new open ocean hybrid coordinate primitive equation model," *Math. Comp. Simul.*, vol. 31, pp. 241–269, 1989.
[25] K. Satnasfield, D. Smeed, G. P. Gasparini, S. McPhail, N. Millard, P. Stevenson, A. Webb, A. Vetrano, and B. Rabe, "Deep-sea, high-resolution, hydrography and current measurements using an autonomous underwater vehicle: The overflow from the Strait of Sicily," *Geophys. Res. Lett.*, vol. 28, pp. 2645–2648, 2001.
[26] K. Sugihara and J. Yuh, "GA-based motion planning for underwater robotic vehicle," in *Proc. 10th Int. Symp. Unmanned Untethered Submersible Technology*, 1997, pp. 406–415.
[27] C. Vasudevan and K. Ganesan, "Case-based path planning for autonomous underwater vehicles," *Autonom. Robots*, pp. 79–89, 1996.
[28] C. W. Warren, "A technique for autonomous underwater vehicle route planning," *IEEE J. Oceanic Eng.*, vol. 15, pp. 190–204, July 1990.

Alberto Alvarez received the M.S. degree in physics in 1991 from the University of Santiago de Compostela, Santiago, Spain, and the Ph.D. degree from the Physics Department, University of Balearic Island, Mallorca, Spain, in 1995. He received a second Ph.D. degree in underwater robotics from the Department of Electrical Engineering, University of Pisa, Pisa, Italy, in 2004.

From 1995 to 1997, he was an Assistant Professor with the University of Balearic Island. He received a postdoctoral position with the Physics Department, National Central University, Taiwan, from 1997 to 1999, to work in underwater acoustics. In 1999, he joined the Department of Rapid Environmental Asssestment, SACLANT Undersea Research Centre, La Spezia, Italy, as a Scientist. Since 2002, he has been a Scientist with the Spanish National Council Research (CSIC), Esporlas.

Andrea Caiti received the Laurea degree in electronic engineering from the University of Genova, Genoa, Italy, in 1988.

From 1989 to 1994, he was a Staff Scientist with the SACLANT Undersea Research Centre, La Spezia, Italy, in the sea-floor acoustics group. In 1994, he joined the Italian University system, with assignments from the Universities of Genova, Pisa, and Siena. He currently is an Associate Professor with the University of Pisa, Pisa, Italy, with teaching assignments in system and control theory, system identification, and industrial automation. Since 2001, he has also been Director of the Italian Interuniversity Center of Integrated Systems for the Marine Environment (ISME). His research interests are focused on inverse problems, data processing, model estimation, and system identification, with applications in the field of robotics and underwater systems.

Reiner Onken received the Ph.D. degree in modeling of the generation and instability of mesoscale fronts from the University of Kiel, Kiel, Germany, in 1986.

After that, he was a Research Assistant with the Hooke Institute, Oxford, U.K., from which he returned to the University of Kiel as an Assistant Professor and Senior Scientist. From 1996 to 2003, he developed strategies for real-time modeling at the SACLANT Undersea Research Centre, La Spezia, Italy. He is with the Institute of Coastal Research (GKSS), Geesthacht, Germany.